Road marking coverage by volcanic ash: an experimental approach

Daniel M Blake[1*], Thomas M Wilson[1], Christopher Gomez[2]

[1] Department of Geological Sciences, University of Canterbury, Private Bag 4800, Christchurch, New Zealand

[2] Department of Geography, University of Canterbury, Private Bag 4800, Christchurch, New Zealand

*Corresponding author
Email: daniel.blake@pg.canterbury.ac.nz

Abstract

Coverage of road markings by volcanic ash is one of the most commonly reported impacts to surface transportation networks during volcanic ashfall. Even minimal accumulation can obscure markings, leading to driver disorientation, diminished flow capacity and an increase in accidents. Such impacts may recur due to repeated direct ashfall (i.e. during prolonged eruptions) and/or due to the re-suspension of ash by wind, water, traffic or other human activities, and subsequent secondary deposition on the road surface. Cleaning is thus required to restore and maintain road network functionality. Previous studies have not constrained ash accumulation measurements to inform road cleaning initiation or plans for safe road operations in environments containing ash. This study uses a laboratory approach with digital image analysis to quantify the percentage of white road marking coverage by three types of volcanic ash with coarse, medium and fine particle size distributions. We find that very small accumulations of ash are responsible for road marking coverage and suggest that around 8% visible white paint or less would result in the road markings being hidden. Road markings are more easily covered by fine-grained ash, with ash area densities of ~30 g m^{-2} (estimated at less than 0.1 mm surface thickness) potentially causing markings to be obscured. For the coarse ash in our study, road marking coverage occurs at area densities of ~1,000 – 2,200 g m^{-2} (~1.0 – 2.5 mm depth) with ash colour and line paint characteristics causing some of the variation. We suggest that risk management measures such as vehicle speed reduction and the initiation of road cleaning activities, should be taken at or before the lower thresholds as our experiments are conducted at a relatively short horizontal distance and the ability to observe road markings when driving will be comparatively reduced.

Highlights

- Image analysis to quantify road marking coverage by volcanic ash.
- Road markings may be obscured when covered by only ~30 g m^{-2} ash.
- Light-coloured ash reduces marking visibility more than dark-coloured ash.
- Thick line paint and retroreflective beads increase susceptibility to coverage.
- Road cleaning is recommended at ~0.1 – 1.0 mm ash surface depths.

Keywords

Stone Mastic Asphalt, visibility, image analysis, road safety, transportation, hazard, impact.

1. Introduction

As populations grow worldwide, more people are residing in volcanically active areas, generally with associated development and expansion of infrastructure including transportation networks (Loughlin et al. 2015). Volcanic ash is the most widely dispersed of all volcanic hazards, often affecting road transport potentially hundreds to thousands of kilometers from its source. Common impacts include reduced skid resistance and visual range, and engine air filter blockage (Wilson et al. 2014). However, perhaps the most frequent and greatest impact during initial ash accumulation is the coverage of road markings. Road marking coverage is also recognised as a substantial impact in areas affected by duststorms, as experienced for example in parts of the Middle East (Aljassar et al. 2006) and North America (ADOT 2015). It is of concern, as much of the visual information needed by a driver to navigate roads safely is provided by continuous road markings (Gibbons et al. 2004). Coverage can lead to driver disorientation (Durand et al. 2001, T.Wilson et al. 2012, USGS 2013) and cascading effects on vehicle movement across the road network, such as diminished flow capacity and an increase in traffic accidents (Wolshon 2009, Blake et al. 2016). For example, the Automobile Association in Australia estimate that if 'average standard' road markings are maintained, the percentage of crash rates is reduced by between 10 and 40%, depending on the crash type (Carnaby 2005).

Road marking coverage by volcanic ash is by no means transient. Impacts may recur due to repeated ashfall (i.e. during prolonged eruptions) and/or due to the re-suspension of ash by wind, water, traffic or other human activities, and subsequent secondary deposition on the road surface. Road cleaning may thus be required to restore and maintain road network functionality. Some authorities (e.g. Kagoshima City Office near Sakurajima volcano, Japan) use road marking coverage as a prompt to mobilise road sweepers and commence ash removal. In 2014 alone when there were 450 eruptions, this led to the removal of 1,274 m^3 of ash from the region's roads (Kagoshima City Office, personal communication, June 08 2015).

Road marking coverage by volcanic ash has been recorded on road networks following a number of eruptions, such as Mt St Helens, USA (1980), Hudson, Chile (1991), Ruapehu, New Zealand (1995-96), Reventador, Ecuador (2002), and during the many ashfall events on Kagoshima City (Japan) from Sakurajima volcano (1955-2015) (Becker et al. 2001, Cole et al. 2005, Leonard et al. 2005, Barnard 2009, Wilson et al. 2009, Magill et al. 2013). However, a review of available sources reveals only limited estimates of volcanic ash thickness that have caused complete coverage, ranging from trace amounts to 5 mm. We suggest that other characteristics, such as the size of ash particles, colour of ash and road surface texture may account for the range to some extent. At such small accumulations however, depths of ash are difficult to measure accurately and other measurements such as the area density of ash may be more appropriate.

In this study at the University of Canterbury's Volcanic Ash Testing Laboratory (VATLab), we adopt a method to replicate volcanic ash deposition on road surfaces by using asphalt slabs painted with two thicknesses of line paint. We employ image classification and segmentation techniques to quantify the extent of road marking coverage by ash and to determine ash depth and surface area density when markings are visually obscured. Based on our findings, suggestions to maintain road safety are made, particularly thresholds for road cleaning initiation.

2. Methods

2.1 Ash and road surface type

Stone Mastic Asphalt (SMA), constructed as 300 x 300 x 45 mm slabs (with aggregate particle size <13.2 mm and a bitumen content of 5.9 %) by the Road Science Laboratory in Tauranga, New Zealand, were placed directly beneath an ash delivery system (section 2.2). Three ash types (a basalt of dark colouration, an andesite of medium colouration, and a rhyolite of light colouration) were sourced from different ash deposits in New Zealand (Table 1) to provide a means of contrast comparison (Blake et al. 2016). As the un-modified samples contained coarse material (some up to 20 mm diameter), all material was dried and then processed using a rock pulveriser and/or sieving to achieve three distinct clusters of

particle size distributions (Figure 1). Spatial distributions of particle sizes from ashfall events are often complex. However, ash particle sizes are typically larger closer to the vent with smaller particles carried further downwind (Jenkins et al. 2014).

Particle sizes (Figure 1) were determined using a Micrometrics Saturn DigiSizer II Laser-Sizer (three runs per sample). We note that the maximum particle sizes for some samples are substantially less than the size of the disc measure used for pulverisation or sieve mesh aperture. For example, the Pupuke basalt sample in the medium particle size group (Table 1) was pulverised with a disc spacing of 990 µm and sieved with a mesh aperture of 1000 µm, but all resulting particles are <500 µm in diameter (Figure 1). This is likely due to the process of pulversiation and mechanism of breakage. Conversely, the maximum particle sizes for some samples are greater than the size of the sieve mesh aperture used (e.g. the fine-grained rhyolite sample, which was sieved at 54 µm but contains a fraction of particles up to 280 µm in diameter). This is due to the tabulate form of some ash particles and their orientation when passing through the sieve.

Table 1. *Ash samples used for testing and their characteristics following processing. Note that there is no coarse particle group for the Hatepe rhyolite ash type due to the smaller particle sizes of the raw field sample.*

	Pupuke, Auckland Volcanic Field			**Poutu, Tongariro**			**Hatepe, Taupo**	
Time of eruption	~200,000 years BP			~11,000 - 12,000 BP			~1,770 years BP	
Ash type	Basalt			Andesite			Rhyolite	
Colour *(determined from Munsell Rock Colour Chart)*	N4: Medium Dark Grey			5Y 6/1: Light Olive Grey (with a small 10YR 6/6 Dark Yellowish Orange component when coarse)			5Y 8/1: Yellowish Grey	
SiO_2 content *(determined by Philips PW2400 XRF analysis)*	44% (mafic)			52% (intermediate)			70% (felsic)	
Dominant minerals *(determined by Philips XRD analysis)*	Diopside, Forsterite, Anorthite			Albite, Augite			Sanidine, Quartz	
Particle size group	coarse	medium	fine	coarse	medium	fine	medium	fine
Modal particle size (µm) (see Figure 1)	680	220	40	540	200	40	180	35
Dry bulk density (g cm^{-3})	1.1	1.5	1.1	1.3	1.2	0.9	0.9	0.7

Mafic ash such as the Pupuke samples, along with intermediate ash such as Poutu, is relatively common from eruptions globally. Eruptions of felsic ash such as Hatepe, are less common (Wicander and Monroe 2006), but the high concentration and quantity of lighter elements, high explosivity and generally high eruption columns, means that the ash can be dispersed up to hundreds of kilometers from the vent (Woo 2009).

Paint is the most common and widespread form of road marking material in most countries worldwide. In this study, Downer Group applied a Damar Bead Lock Oil Based Paint, which contains 63% solids, using a standard machine on the asphalt concrete slabs. The side of one slab was painted with a single coat 180-200 µm thick, and the other side with four coats (720-800 µm thick in total) to replicate markings that have been exposed to different abrasion or multiple paint applications. The other slab was painted with the same thickness lines but with retroreflective glass beads incorporated in the paint mix.

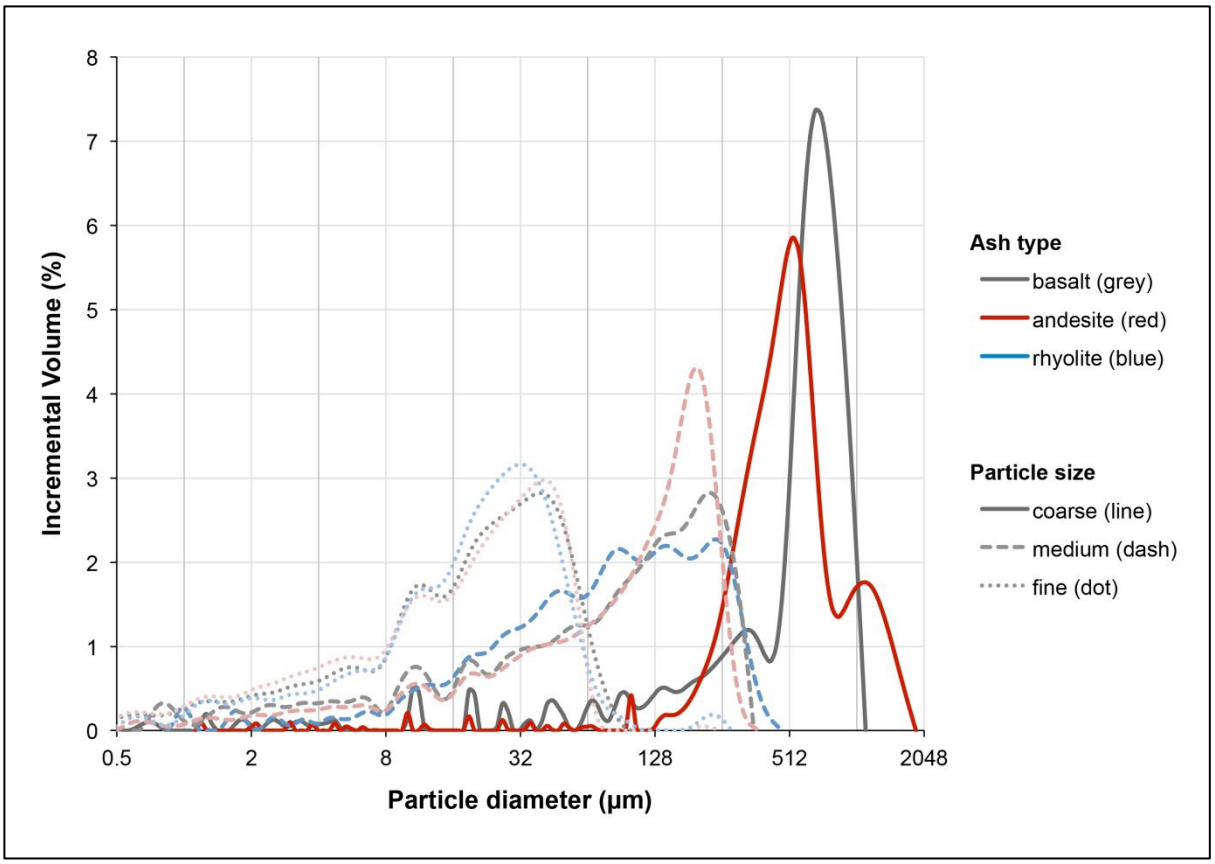

Fig. 1 *Mean particle size distributions of samples used in experimentation and their designated classification discussed in this article (i.e. coarse, medium and fine).*

2.2 Ash application and measurement

The ash delivery system used comprises of a 400 x 400 x 100 mm sieve box with an adaptable mesh base (of 1 mm, 500 µm or 125 µm aperture depending on the particle size distribution of the ash) and manual-striking hammer which causes ash to fall through when struck. The set-up has been used in previous experiments including by G.Wilson et al. (2012) and Hill (2014). The ash delivery system produces ash in a consistent and repeatable manner and is calibrated to replicate ash settling velocities and accumulation rates that would be expected from real ashfalls. The delivery system has been designed using formulas derived from Bonadonna et al. (1998) (equations 1-3) to ensure that the majority of ash particles dispensed from the sieve box reach terminal velocity well before ground level (Hill 2014):

$$V_t \approx (3.1\, g\, \rho\, d\, /\, \sigma)^{1/2} \quad (1)$$

$$V_t \approx (g\, \rho\, d^2\, /\, 18\, \mu) \quad (2)$$

$$Vt \approx d\, (4\rho^2\, g^2\, /\, 225\, \mu\, \sigma)^{1/3} \quad (3)$$

Where V_t is the terminal velocity, g is the acceleration due to gravity (9.81 m s^{-2}), ρ is the density of the particles, d is the particle diameter, σ is the density of the air and µ is the dynamic viscosity of the medium (Bonadonna et al. 1998, Hill 2014).

In this study, we incorporate the ash delivery system to investigate failure thresholds (i.e. when road markings become obscured by ash). Petri dishes (85 mm in diameter) were placed on the asphalt surface at the end of each road marking line to enable measurements of ash thickness from a flat surface (using a calliper). Ash thicknesses within asphalt aggregate pores of both average and distinctively large depth, and from the top of aggregate grains were also recorded (averaged from 5 measurements for each). Furthermore, the mass of ash collected in the petri dishes was measured at each stage in order to calculate the area density throughout experimentation. This was conducted to allow a more accurate measure of ash deposition, particularly as the thickness of ash at low accumulations is difficult to

measure, and also the quantity of ash released by the delivery system experiences slight variations between ash types and as the experiment progresses and sieve mesh becomes clogged.

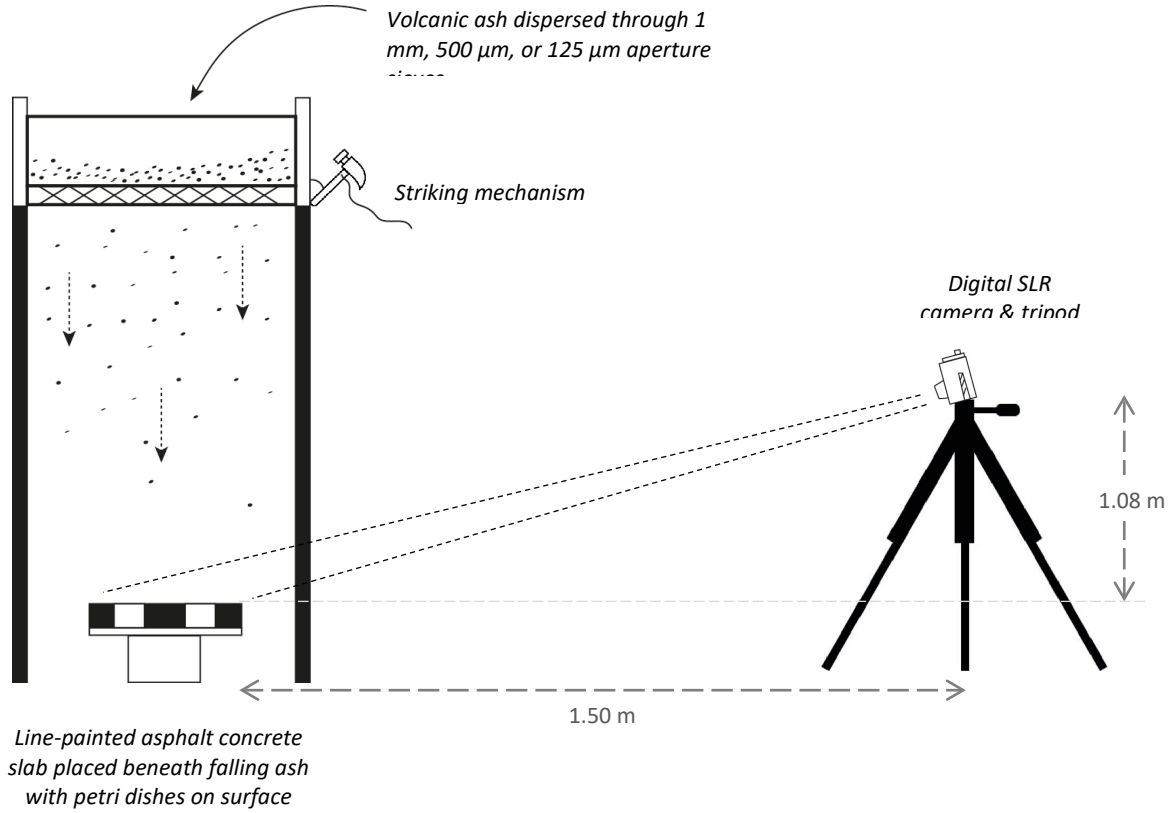

Fig. 2 *Experimental set-up for road marking visibility testing (adapted from Blake et al. 2016).*

2.3 Image collection

A Fuji Finepix S100 (FS) digital SLR camera was mounted on a tripod 1.5 m horizontally and 1.08 m vertically away from the slab (Figure 2), 1.08 m being the height of the driver's eye above the road in measuring stopping sight distances (Fambro et al. 1997, Blake et al. 2016). A digital photograph was taken at a focal length of 200 mm (under consistent camera and light conditions) and observations were noted following strikes of the ash delivery system after the ash had settled. This was conducted until five photos after the ash visually appeared to the observer to completely cover the markings. The number of strikes between each photo was varied depending how readily the ash sample passed through the sieve mesh. The mean depths of ash in the asphalt pores and on the surfaces of both the asphalt slab and petri dishes, along with the mass of petri dishes containing ash were measured and recorded in conjunction with each photo.

Other research involving road marking visibility has been conducted in the past, often involving participant drivers in simulated driving conditions (e.g. Brooks et al. 2011) or on the road at specialised road research facilities (e.g. Gibbons et al. 2004, Gibbons and Williams 2012). Specialised technical equipment has also been developed to measure the retroreflective luminance of markings (e.g. Carlson and Miles 2011). Most previous experiments have assessed the effectiveness of road markings where atmospheric conditions such as rainfall and fog present a hazard to driving. In these experiments, the distance between participants or equipment from road markings is often in the order of tens of meters. Our experimental set-up enables precise analysis of ash accumulation on the road surface and detailed measurements under controlled conditions. We investigate road markings at close range (1.5 m horizontal distance) and, due to spatial laboratory constraints, do not directly account for viewing road markings >1.5 m away. Additionally, we do not account for visibility interference due to airborne volcanic ash, which requires separate investigation. Therefore, our results for road marking coverage are

conservative, and at greater viewing distances or where the atmosphere contains ash, road marking visibility will likely be even less than portrayed.

2.4 Image analysis

Each image file was opened using Ilastik version 0.5.12 software (Sommer et al. 2011) to conduct supervised segmentation by pixel colour; one class was created for the white paint, and another class for ash or asphalt (Figure 3) (Blake et al. 2016). After segmentation (which displayed the white paint as red, and asphalt and ash as green), image registration was achieved in Adobe Photoshop version CS6, ensuring that each image was cropped automatically without the geometry of objects changing between images. The photographs were intentionally not nadir, and the images were not orthorectified as the viewing angle and associated properties of visibility were of particular interest in the study. The mean pixel resolution was 1 pixel to 0.088 mm for the cropped area of the photographs. A fuzziness setting of 200 was selected to account for the range of colours in the ash, asphalt and line paint. This selects all pixels that are the exact same colour as the pixels clicked on, as well as all pixels that are within 200 brightness values lighter or darker. The 'histogram' function was then used to observe and record the pixel count for the white paint (red pixels). The number of pixels for the ash/asphalt was then calculated by subtracting the number for the white paint from the total pixel count. A total of 142 photographs (i.e. 284 cropped line images) were analysed with a mean of nine images analysed for each sample of specific particle size distribution and ash type.

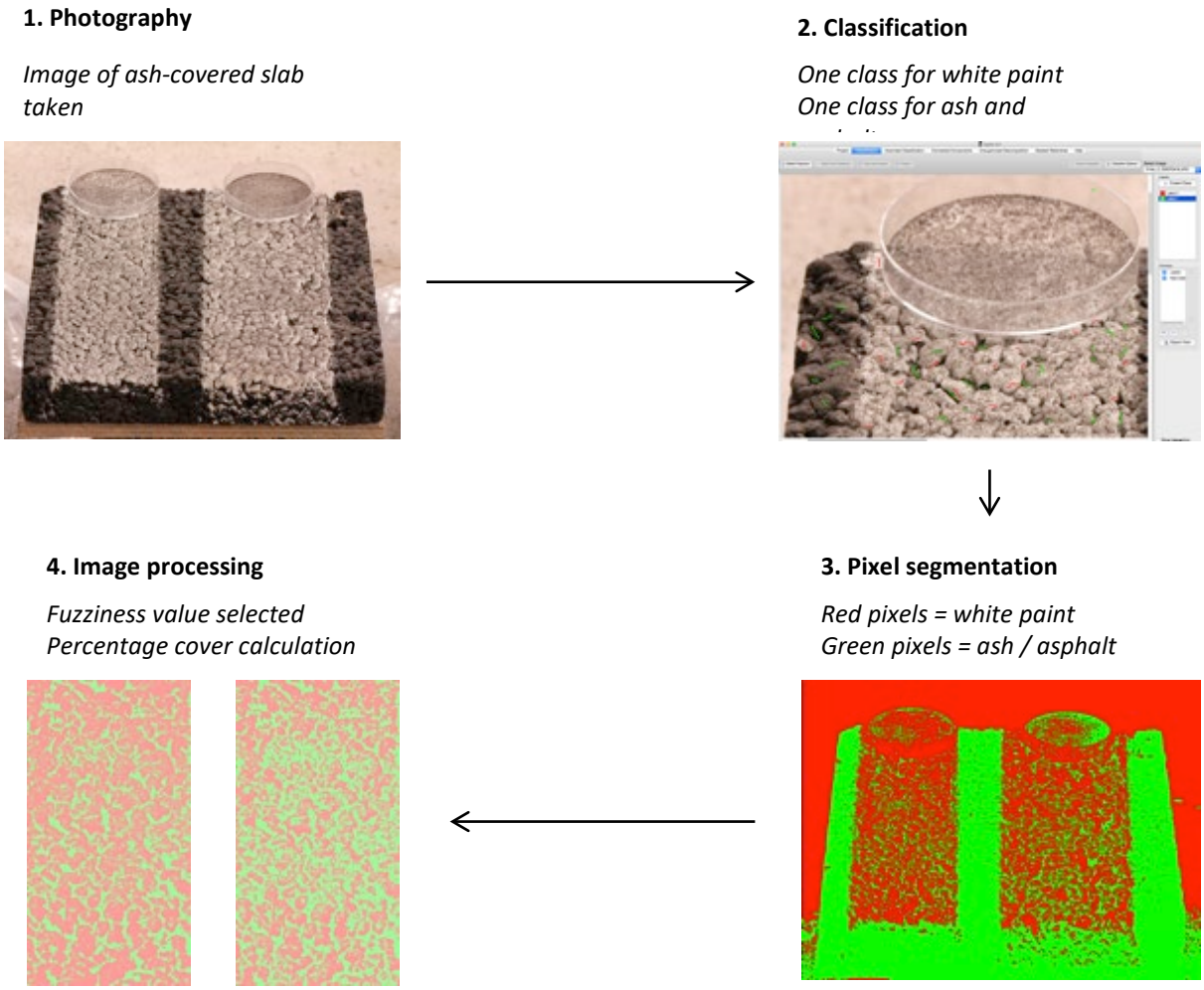

Fig. 3 *Generalised steps for the image analysis process.*

3. Results and discussion

After the sieve box had been struck <5 times, the subsequent dispersal of ash through the delivery system and accumulation on the slabs led to a substantial decrease in the percentage of pixels representing white road marking paint for all of our samples (Figure 4). This suggests that only very small ash accumulations are required for an impact on road marking visibility reduction (Blake et al. 2016). With further ash accumulation, the road markings continue to become obscured but at a decreasing rate. Through physical visual observations in the laboratory and comparisons with raw and analysed images (section 2.4), it was decided that when 8% white line paint or less is visible that it would be unlikely that drivers could effectively view road markings when driving (Blake et al. 2016). Therefore, the measurements of ash area density and depth at this threshold are of interest. It appeared particularly difficult to delineate the edges of the markings around this value, although we note that the 8% threshold is somewhat subjective and that there are few comparative studies; most others adopt instruments such as retroreflectometers which are used over several tens of meters (e.g. Dravitzki et al. 2003, Babic et al. 2014).

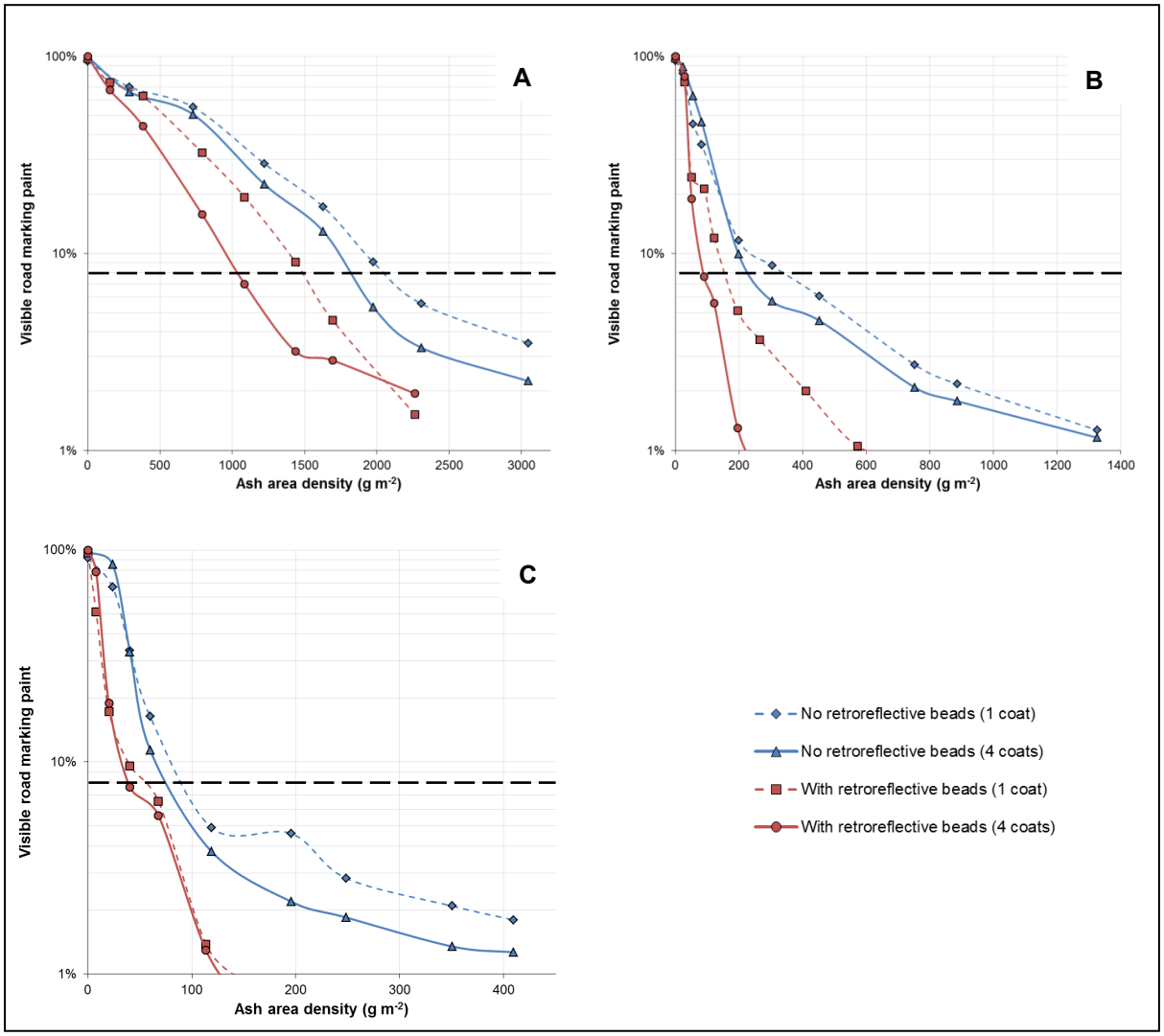

Fig. 4 *Percentage of white road marking paint visible and ash area densities for the andesite sample with mode particle size of a) 600 µm, b) 200 µm, and c) 40 µm. The results for asphalt slabs covered by one and four coats of paint with and without retroreflective glass beads incorporated in the paint mix are shown. Also displayed are the thresholds for 8% visible road marking paint (horizontal black dashed lines). We suggest that it would be difficult for drivers to view road markings at or below this threshold.*

The 8% threshold of pixels for white paint (i.e. 92% pixels for ash/asphalt) was evident through image analysis at ash area densities of between 30 g m^{-2} and 2,150 g m^{-2} for all ash samples used in experimentation (Table 2). This equates to ash depths of between trace amounts (taken to be <0.1 mm in

our study) and 2.2 mm, measured from the surface of the asphalt aggregate. The large range in measurements is largely due to the influence of particle size, but also ash type and road paint characteristics to some degree (sections 3.1 – 3.3).

Our findings correspond well with the ash characteristics and observations of road marking coverage at Sakurajima volcano in Kyushu, Japan. In June 2015, the Kagoshima City Office reported that area densities were currently ~300-400 g m^{-2} when road markings could not be seen and cleaning was required (Kagoshima City Office, personal communication, June 08 2015). The ash is typically of andesitic type, typically with a SiO_2 content of ~59%, and mode particle sizes of 150-200 μm at this distance (4-5 km) for recent eruptions from the Showa crater (Yamanoi et al. 2008, Matsumoto et al. 2013, Nanayama et al. 2013, Miwa et al. 2015). Our summarised results (Table 2) suggest that ash depths on the roads, measured from the surface of the asphalt aggregate, would have been approximately 0.5 mm at the time.

Table 2. *Measurements of ash area density and depths when it would be difficult for drivers to see road markings (i.e. when 8% white line marking paint was visible), determined through image analysis for all of the ash samples tested. The range of values is largely due to differences in paint thickness (i.e. number of coats) and retroreflective bead content of the paint (see section 3.3), as well as unavoidable but natural variations in surface texture across the asphalt slabs.*

		ASH TYPE		
		Basalt	**Andesite**	**Rhyolite**
MODE PARTICLE SIZE DISTRIBUTION	**Coarse (600 – 700 μm)**	Area density: 1350 – 2150 g m^{-2} Depth on surface: 1.0 – 2.2 mm Depth in voids: 3.3 – 7.5 mm	Area density: 1050 – 2100 g m^{-2} Depth on surface: 1.0 – 1.4 mm Depth in voids: 3.2 – 7.5 mm	*(No data as sample not possible at this particle size)*
	Intermediate (200 – 260 μm)	Area density: 240 – 450 g m^{-2} Depth on surface: 0.3 – 0.8 mm Depth in voids: 0.9 – 1.5 mm	Area density: 80 – 350 g m^{-2} Depth on surface: 0.2 – 0.5 mm Depth in voids: 0.4 – 1.5 mm	Area density: 40 – 180 g m^{-2} Depth on surface: 0.2 – 0.4 mm Depth in voids: 0.2 – 0.7 mm
	Fine (35 – 45 μm)	Area density: 45 – 80 g m^{-2} Depth on surface: trace – 0.1 mm Depth in voids: trace – 0.1 mm	Area density: 35 – 80 g m^{-2} Depth on surface: trace – 0.1 mm Depth in voids: trace – 0.1 mm	Area density: 30 – 65 g m^{-2} Depth on surface: trace – 0.1 mm Depth in voids: trace – 0.1 mm

We highlight the importance of outlining the specifics for depth type measured on road surfaces for ash accumulations less than ~10 mm. Depths within the asphalt aggregate voids were found to be over five times greater than those measured from the surface of the aggregate in some cases (e.g. for the coarse andesite, ash depths within voids were ~7.5 mm when surface depths were ~1.4 mm).

3.1 Road marking type

The thickness of surface paint appears to have some influence on road marking coverage. Figure 4 illustrates that the lines with four coats of paint generally become covered more easily than a single coated line. This is intuitive because the greater quantity of paint acts to reduce the macrotexture of the asphalt surface, causing the voids to fill sooner with the same mass of ash.

The markings of paint that incorporate retroreflective glass beads in the mix are generally more easily obscured. This is perhaps due to the retroreflective beads adding to the overall volume of paint, thus reducing the macrotextural depth of the asphalt voids. The rougher microtexture may cause more ash to remain on the surface than for road markings without beads (caused by retroreflective beads 'trapping' individual ash particles as they fall). Crystalline ash particles will also act to reflect light, potentially reducing the effectiveness of the added retroreflective beads. Therefore, although retroreflective beads are added to paint with the overall intention of improving road safety, they act to reduce the visibility of road markings when volcanic ash accumulates, reducing road safety in such environments.

The ranges of ash area densities and ash depths shown in Table 2 are mainly due to the variations in road marking characteristics. Generally, the higher values reflect conditions where there is less paint and/or where the paint mix does not contain retroreflective beads, and the lower values in the table correspond to road markings formed of multiple paint layers (with little wear) and/or where the paint incorporates retroreflective beads.

3.2 Ash particle size

It is evident that road marking coverage is highly dependent on the particle size distribution of volcanic ash falling on textured road surfaces such as SMA (Table 2). Ash depth measurements in petri dishes and on different locations of the asphalt surfaces, and through visual observations when the ash was falling, revealed that this is largely due to the behaviour of individual particles upon impact (Figure 5).

A mass of fine ash particles is more effective at covering road markings than the same mass of coarse particles. Indeed, for our samples the mass of the ash in petri dishes when the road markings became covered (i.e. when only 8% white line paint was visible) ranged from 0.2 g (for fine-grained particles) to 14 g (for coarse-grained particles). This is largely because coarser particles bounce into the macrotextural voids of the asphalt aggregate and initially accumulate in these spaces, with white road marking paint on the upper asphalt surface remaining uncovered and visible to drivers (Figure 5). Even as the ash in the void spaces accumulates to the upper surface of the asphalt, ash particles settling on the surface of the aggregate have a tendency to be displaced by further ash that falls and collect in areas immediately above the voids where the thicker existing ash limits movement. This results in very small mounds of ash immediately above the voids (with white line paint still visible in-between) before ash spreads across the entire surface of the asphalt.

Fine ash particles pack more densely wherever they settle, causing the surface to be easily covered. This process is observed on the asphalt and on the flat surfaces of our petri dish bases. It has also recently been attributed to the vulnerability of horizontally placed photovoltaic modules and power-output reduction (Zorn and Walter 2016). Furthermore, the fine ash particles appear to exhibit electrostatic properties and adhere more readily to the asphalt surface, successfully covering the line-covered aggregate at various orientations. Ash with finer particle size distributions, and sometimes more triboelectrically charged particles (Aplin et al. 2014) are relatively common in distal volcanic plumes. Therefore, our findings indicate that road marking coverage, especially in distal locations from volcanic vents, should not be overlooked.

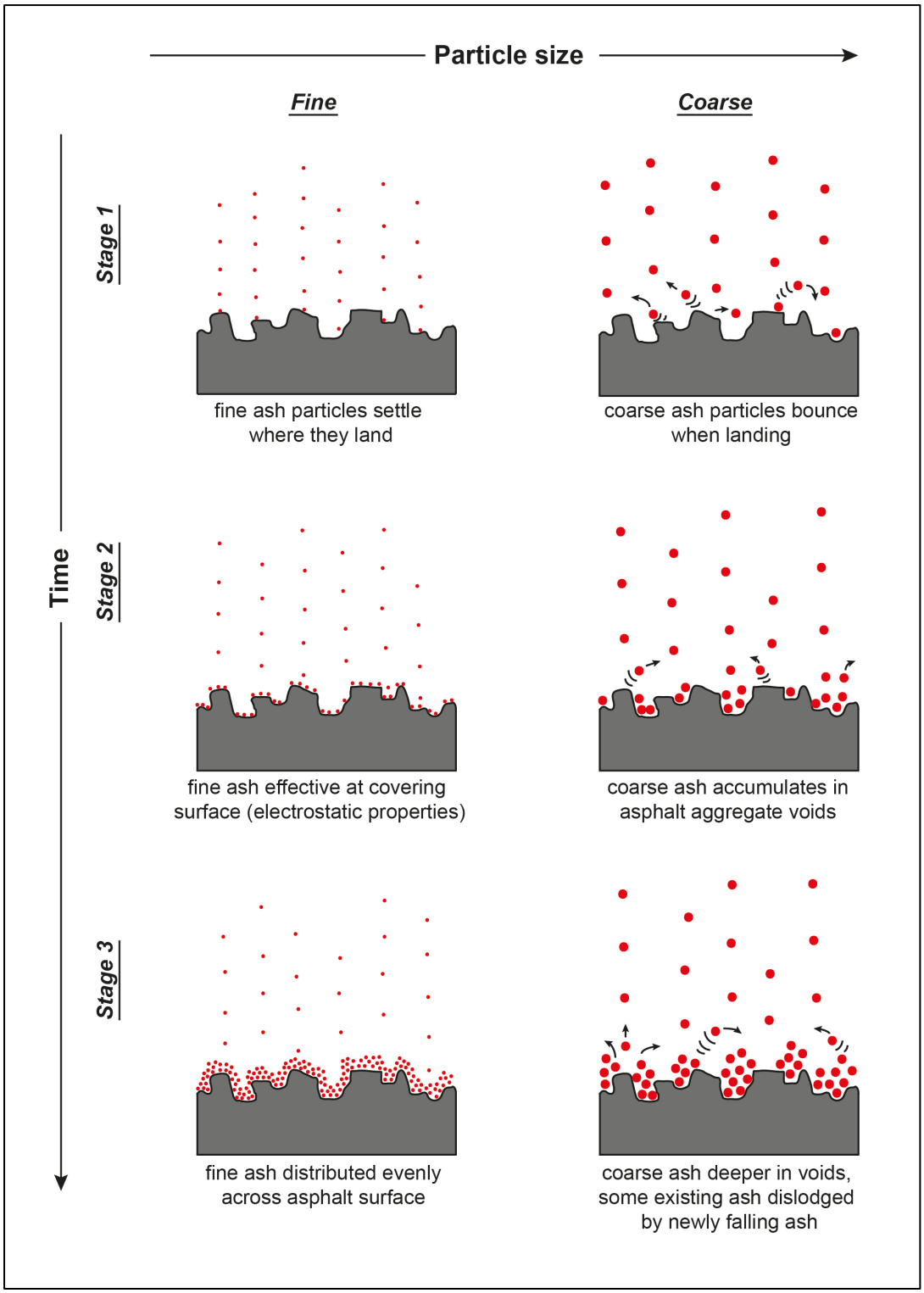

Fig. 5 *The process of ash accumulation on textured road surfaces showing the difference between ash containing predominantly fine and coarse particles.*

3.3 Ash type and contrast

Although the mean dry bulk densities for the light-coloured ash were less than those of the darker material, less ash is required at intermediate and coarse particle sizes to cover the same percentage of road markings. For example, at intermediate particle sizes (i.e. 200-260 μm modal distributions), 8% of line paint is visible at mean asphalt surface accumulations of 0.55 mm for the basalt (dark-coloured), 0.35

mm for the andesite (mid-coloured), and 0.30 mm for the rhyolite (light-coloured) (Figure 6). This suggests that white road markings covered by light-coloured deposits such as the rhyolite may become obscured at smaller depths than dark-coloured deposits such as the basalt. Although the same trend is suspected for fine ash particle sizes, it is not verified here due to the very small accumulations it took for surfaces to be covered (≤ 0.1 mm) and difficulties in measuring and estimating ash depths.

Some of the difference between ash colour types may be due to errors in the image analysis process whereby the ash and markings are more difficult to classify when the ash is of lighter colour. However, the image analysis findings correspond with the visual observations recorded during experimentation in that it was more difficult to distinguish road markings when covered by light-coloured ash compared to the same depths of dark-coloured ash (Blake et al. 2016). The findings also align with the mere definition of visual contrast (i.e. the difference in colour or brightness between objects that makes them distinguishable). With light-coloured ash covering the dark asphalt either side of white road markings; the markings will be less distinguishable. Additionally, the farther an object is from a driver, the greater the contract requirements (Gibbons et al. 2004). Therefore a driver's ability to see road markings with distance may be less for light-coloured than dark-coloured ash (Blake et al. 2016).

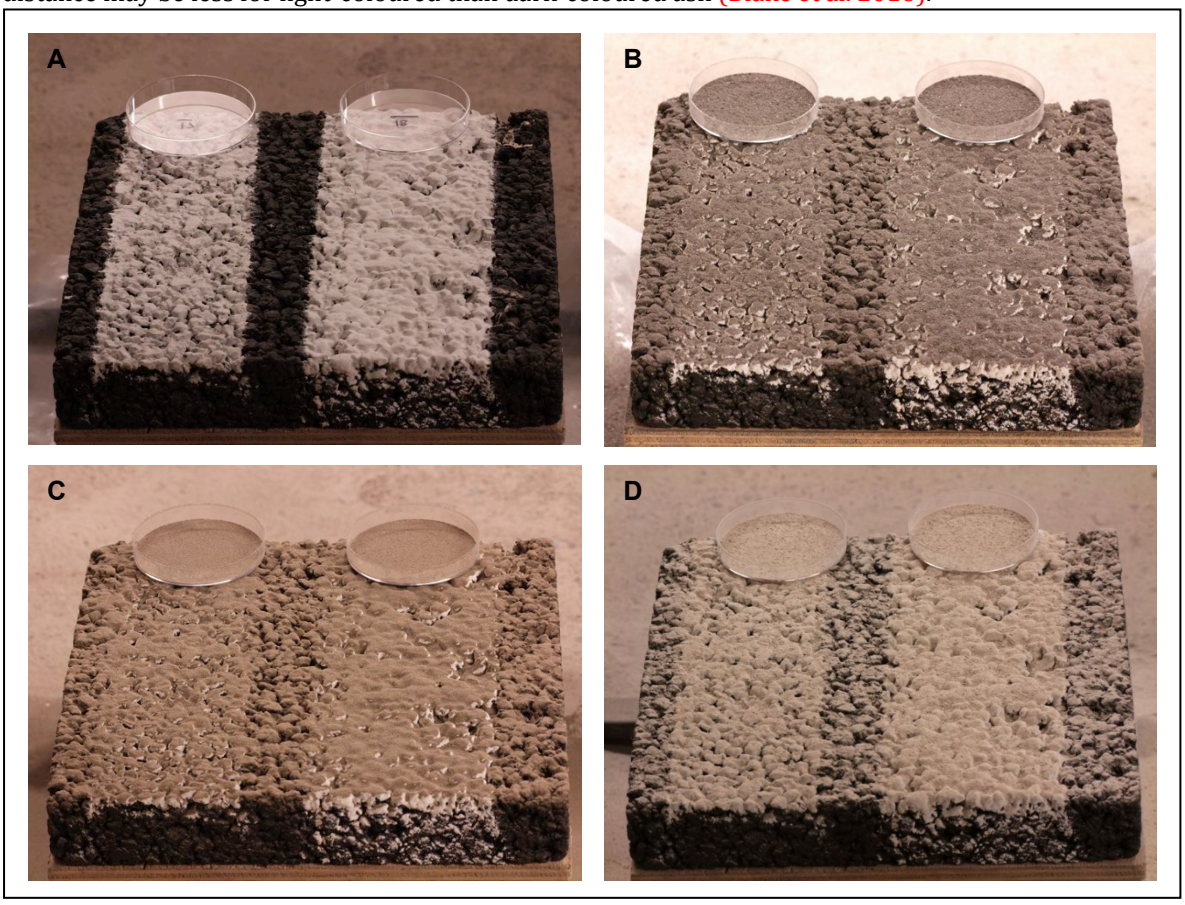

Fig. 6 *Road markings painted on a SMA slab as one coat (left lines) and four coats (right lines), both containing no retroreflective beads in the paint mix (adapted from Blake et al. 2016). a) shows the markings with no volcanic ash on the surface. b), c) and d) show when ≤ 8% of line paint is visible (i.e. when it would be difficult for drivers to see the lines) for basaltic, andesitic and rhyolitic ash of 200-260 µm modal particle size distributions respectively. This corresponds to mean thicknesses on the surface of the asphalt aggregate of 0.55 mm for the basalt, 0.35 mm for the andesite, and 0.30 mm for the rhyolite.*

4. Conclusion

Our experimental findings demonstrate that very low levels of volcanic ash accumulation can cause substantial road marking coverage. If ash particles are predominantly fine (i.e. mode particle sizes ≤45

μm), then road markings may become obscured for drivers when ash area densities are between 30 and 80 g m^{-2}. This is equivalent to ≤0.1 mm of ash accumulation on the surface of the asphalt.

Ash particle size distribution is likely the most important characteristic for road marking coverage at small depths and a mass of fine particles is much more effective at covering a surface than the same mass of coarse particles. This is largely attributed to the ash particle behaviour upon initial impact, with coarse particles bouncing into voids between the asphalt aggregate and fine particles generally settling where they initially land. For coarse (i.e. mode particle sizes ≥600 μm) ash, depths ≥1.0 mm, measured from the surface of the aggregate, or ≥3.2 mm, measured within the asphalt voids, lead to road marking coverage. This represents ash area densities at least 13 times greater than for fine ash of the same type.
These thresholds assume dry and near-pristine atmospheric conditions (i.e. no airborne ash) and further work is required to determine the extent of visual range impairment by suspended ash particles.

Road markings covered by light-coloured ash of the same thickness as dark-coloured ash are more difficult to distinguish (due to low contrast). Multiple paint layers (assuming little wear) and paint mix that incorporates retroreflective glass beads also make markings more difficult to distinguish when covered by ash. Although crucial to consider on all road networks that include line painted surfaces in volcanically active regions, our findings especially highlight the susceptibility of road markings being covered in distal areas from the vent.

We recommend thresholds for when road cleaning should occur on asphalt surfaces in order to maintain road safety and network functionality. Note that the values assume 'worse-case conditions' for volcanic ash coverage in terms of paint characteristics:

- For fine (~30 – 45 μm mode particle size) ash of all types and felsic ash such as rhyolite up to a size dominated by ~300 μm particles, road cleaning should be conducted at or before ash area densities of 30 – 45 g m^{-2}. Depths will be extremely difficult to measure at such accumulations but will likely be around 0.1 – 0.2 mm from the surface of the upper aggregate.
- For intermediate size (up to ~300 μm mode particle size) andesite, road cleaning should be conducted at ash area densities of ~100 g m^{-2}. For mafic ash such as basalt of the same size, it should be conducted at ~250 g m^{-2}. Surface depths will be around 0.2 – 1.0 mm at this stage.
- For coarse (mode particle sizes up to ~800 μm) andesite and basalt, road cleaning should occur at ash area densities of ~1,000 and 1,500 g m^{-2} respectively, which is equivalent to surface depths of approximately 1.0 – 2.5 mm.

Due to road safety considerations in environments when there is no volcanic ash, it seems counterintuitive to suggest changes to road marking paint mix properties such as changes in retroreflective glass bead concentrations or design, so that visibility of road markings is maintained at a higher standard solely during ashy conditions. Therefore, we do not suggest that any major changes to physical road marking properties should be made in areas prone to volcanic ashfall. Applying new coats of paint should only be conducted if existing paint is sufficiently worn and if it is required to improve road safety in normal conditions. This is because thicker paint can lead to road markings becoming more easily obscured by ash. Changes to the physical structure of the road surface itself, such as the application of an aerodynamic profile to promote particle removal from the carriageway by wind-driven saltation (as achieved in Kuwait (Aljassar et al. 2006)), may be cost-effective in some regions frequently affected by volcanic ash. However, perhaps the simplest technique to improve road safety in all areas when road markings become covered is for all drivers to travel at a reduced speed, or to avoid driving until the ash is cleared.

Acknowledgements

We thank the University of Canterbury Mason Trust scheme, New Zealand Earthquake Commission (EQC) and Determining Volcanic Risk in Auckland (DEVORA) project for their financial support towards the study through the provision of funding for authors Daniel Blake and Thomas Wilson. We also express thanks for the support towards laboratory assistance and equipment provided by several people, whose help was vital to the success of this study. In particular we wish to thank Janet Jackson and Howard

Jamison of Downer Group for coordinating the painting of the asphalt concrete slabs, and Kerry Swanson, Matt Cockcroft, Chris Grimshaw, Stephen Brown, Alec Wild, Connor Jones and Brigitt White for their assistance with sample preparation and conducting experiments at the University of Canterbury's Volcanic Ash Testing Lab. Daniel Blake would also like to thank his PhD co-supervisors, Jim Cole (University of Canterbury), Jan Lindsay (The University of Auckland) and Natalia Deligne (GNS Science) for their edits, guidance and support throughout the project.

References

ADOT (2011) Dusty roads. Arizona Department of Transportation Blog. http://www.azdot.gov/media/blog/posts/2011/04/18/dusty-roads Accessed 13/10/2015.

Aljassar, A.H. Al-Kulaib, A. Ghoneim, A.N. Metwali, E-S. (2006) A cost effective solution to the problem of sand accumulation on a desert road in Kuwait. Third Gulf Conference on Roads, March 6-8, 2006. www.draljassar.net/text/t0026.doc Accessed 13/10/2015.

Aplin, K. Houghton, I. Nicoll, K. Humphries, M. Tong, A. (2014) Electrical charging of volcanic ash. Proceedings ESA Annual Meeting on Electrostatics. http://www.electrostatics.org/images/ESA_2014_G_Aplin_et_al.pdf Accessed 20/01/2016.

Babic, D. Fiolic, M. Prusa, P. (2014) Evaluation of road markings retroreflection measuring methods. European Scientific Journal, 3, pp.105-114.

Barnard, S.T. (2009) The vulnerability of New Zealand lifelines infrastructure to ashfall. Doctor of Philosophy Thesis, Department of Geological Sciences, University of Canterbury, Christchurch, New Zealand.

Becker, J. Smith, R. Johnston, D. Munro, A. (2001) Effects of the 1995-1996 Ruapehu eruptions on communities in central North Island, New Zealand, and people's perceptions of volcanic hazards after the event. The Australasian Journal of Disaster and Trauma Studies, 2001-1.

Blake, D.M. Wilson, T.M. Deligne, N.I. Lindsay, J.L. Cole, J.W. (2016) Impacts of volcanic ash on road transportation: considerations for resilience in central Auckland. Proceedings Paper for the Institute of Professional Engineers New Zealand (IPENZ) Transportation Group Conference (March 2016), Auckland, New Zealand.

Carlson, P. Miles, J. (2011) Nighttime visibility of in-service pavement markings, pavement markers, and guardrail delineation in Alaska (with and without continuous lighting). Alaska Department of Transportation, Statewide Research Office, Juneau, Alaska. http://www.dot.state.ak.us/stwddes/research/assets/pdf/fhwa_ak_rd_11_04.pdf Accessed 26/09/2015.

Carnaby, B. (2005) Road marking is road safety. Conference paper by Potters Asia Pacific, presented at the New Zealand Roadmarkers Federation Conference 2005, Christchurch, New Zealand.

Cole, J.W. Sabel, C.E. Blumenthal, E. Finnis, K. Dantas, A. Barnard, B. Johnston, D.M. (2005) GIS-based emergency and evacuation planning for volcanic hazards in New Zealand. Bulletin of the New Zealand Society for Earthquake Engineering, 38:2, pp.149-164.

Dravitzki, V.K. Wood, C.W.B. Laing, J.N. Potter, S. (2003) Guidelines for performance of New Zealand markings, Opus Central Laboratories Report 03-527605, http://www.nzta.govt.nz/assets/resources/guidelines-for-performance-of-nz-road-markings/docs/guidelines-for-performance-of-nz-road-markings.pdf Accessed 25/01/2016.

Durand, M. Gordon, K. Johnston, D. Lorden, R. Poirot, T. Scott, J. Shephard, B. (2001) Impacts and responses to ashfall in Kagoshima from Sakurajima Volcano – lessons for New Zealand. GNS Science Report 2001/30, 53 p.

Fambro, D.B. Fitzpatrick, K. Rodger, J.K. (1997) Determination of stopping sight distances. National Cooperative Highway Research Program Report 400, Transportation Research Board National Research Council, Washington D.C.

Gibbons, R.B. Hankey, J. Pashaj, I. (2004) Wet night visibility of pavement markings: executive summary. Virginia Tech Transportation Institute, Virginia Polytechnic Institute and State University, Charlottesville, Virginia. https://vtechworks.lib.vt.edu/bitstream/handle/10919/46697/05-cr4.pdf?sequence=1 Accessed 26/09/2015.

Gibbons, R.B. Williams, B.M. (2012) Assessment of the durability of wet night visible pavement markings: wet visibility project phase IV. Virginia Centre for Transportation Innovation and Research, Charlottesville, Virginia. http://www.virginiadot.org/vtrc/main/online_reports/pdf/12-r13.pdf Accessed 26/09/2015.

Hill, D.J. (2014) Filtering out the ash: mitigating volcanic ash ingestion for generator sets. Master of Science Thesis, Department of Geological Sciences, University of Canterbury, Christchurch, New Zealand.

Jenkins, S.F. Wilson, T.M. Magill, C.R. Miller, V. Stewart, C. Marzocchi, W. Boulton, M. (2014) Volcanic ash fall hazard and risk: technical background paper for the UN-ISDR 2015 Global Assessment Report on Disaster Risk Reduction. Global Volcano Model and IAVCEI. www.preventionweb.net/english/hyogo/gar Accessed 08/01/2016.

Leonard, G.S. Johnston, D.M. Williams, S. Cole, J.W. Finnis, K. Barnard, S. (2005) Impacts and management of recent volcanic eruptions in Ecuador: lessons for New Zealand. GNS Science Report 2005/20, 52 p.

Loughlin, S.C. Sparks, R.S.J. Brown, S.K. Jenkins, S.F. Vye-Brown C. (2015) Global Volcanic Hazards and Risk, Cambridge University Press, UK.

Matsumoto, A. Nakagawa, M. Amma-Miyasaka, Iguchi, M. (2013) Temporal variations of the petrological features of the juvenile materials during 2006 to 2010 from Showa crater, Sakurajima volcano, Kyushu, Japan. Bulletin of Volcanology, 58:1, pp.191-212.

Miwa, T. Shimano, T. Nishimura, T. (2015) Characterization of the luminance and shape of ash particles at Sakurajima volcano, Japan, using CCD camera images. Bulletin of Volcanology, 77:5, 13p.

Magill, C. Wilson, T. Okada, T. (2013) Observations of tephra fall impacts from the 2011 Shinmoedake eruption, Japan. Earth Planets Space, 65, pp.677-698.

Nanayama, F. Furukawa, R. Ishizuka, Y. Yamamoto, T. Geshi, N. Oishi, M. (2013) Chracterization of fine volcanic ash from explosive eruption from Sakurajima volcano, South Japan, American Geophysical Union Fall Meeting 2013, December 2013.

Sommer, C. Strähle, C. Köthe, U. Hamprecht, F.A. (2011) Ilastik: interactive learning and segmentation toolkit. BibTex file, Technical Report, In: Eighth IEEE International Symposium on Biomedical Imaging Proceedings, pp.230-233.

USGS (2013) Volcanic ash: effects and mitigation strategies. United States Geological Survey http://volcanoes.usgs.gov/ash/trans/ Accessed 21/09/2015.

Wilson, T.M. Cole, J.W. Stewart, C. Cronin, S.J. Johnston, D.J. (2011) Ash storms: impacts of wind-remobilised volcanic ash on rural communities and agriculture following the 1991 Hudson eruption, southern Patagonia, Chile. Bulletin of Volcanology, 73, pp.223-239.

Wilson, G. Wilson, T. Cole, J. Oze, C. (2012) Vulnerability of laptop computers to volcanic ash and gas. Natural Hazards, 63:2, pp.711-736.

Wilson, T.M. Stewart, C. Sword-Daniels, V. Leonard, G.S. Johnston, D.J. Cole, J.W. Wardman, J. Wilson, G. Barnard, S.T. (2012) Volcanic ash impacts on critical infrastructure. Physics and Chemistry of the Earth, 45-46, pp.5-23.

Wolshon, B. (2009) Transportation's role in emergency evacuation and re-entry: a synthesis of highway practice. National Cooperative Highway Research Program, Transportation Research Board Synthesis 392, Washington D.C.

Wicander, R. Monroe, J. (2006) Essentials of Geology: fourth edition. Thomson Brooks/Cole, United States of America.

Woo, G. (2009) A new era of volcano risk management: RMS special report. Risk Management Solutions, Inc. London, UK.

Yamanoi, Y. Takeuchi, S. Okumura, S. Nakashima, S. Yokoyama, T. (2008) Color measurements of volcanic ash deposits from three different styles of summit activity at Sakurajima volcano, Japan: conduit processes recorded in color of volcanic ash. Journal of Volcanology and Geothermal Research, 178, pp.81-93.

Zorn, E. Walter, T.R. (2016) Influence of volcanic tephra on photovoltaic (PV)-modules: an experimental study with application to the 2010 Eyjafjallajökull eruption, Iceland. Journal of Applied Volcanology, 5:2, pp.1-14.